From fibers to satellites: lessons to learn and pitfalls to avoid when optical communications move to long distance free space

A. Vannucci
University of Parma
Parma, Italy
armando.vannucci@unipr.it

T. Foggi
University of Parma
Parma, Italy
tommaso.foggi@unipr.it

A. Zahr
DLR, German Aerospace Centre
Oberpfaffenhofen, Germany
ayman.zahr@dlr.de

H. Chougrani
SnT, University of Luxembourg
Luxembourg, Luxembourg
houcine.chougrani@uni.lu

B. Matuz
DLR, German Aerospace Centre
Oberpfaffenhofen, Germany
balazs.matuz@dlr.de

Bhavani Shankar M. R
SnT, University of Luxembourg
Luxembourg, Luxembourg
bhavani.shankar@uni.lu

G. Colavolpe
University of Parma
Parma, Italy
giulio.colavolpe@unipr.it

***Abstract*—The paper summarizes the recent investigation on feasibility of adapting state-of-the-art coherent fiber-optics (FO) systems for Free Space Optical (FSO) scenarios. This investigation is critically dependent on the intertwined aspects of architecture, as well as device and propagation impairments (including the channel) appearing in the aforementioned systems. Towards this, the work identified the key system differences between the two systems. Particularly, the FSO channel model was investigated, impact of atmospheric turbulence on FSO was discussed and a channel series was generated. Subsequently, relevant FO techniques including coherent detection, wavelength division multiplexing and Time-Frequency packing (TFP) were reviewed. Another departure from FSO works was the emphasis on coherent reception; receiver architectures and diversity schemes were first investigated. The former strived to make fair comparison amongst the receivers considering the diverse nature of perturbation added, while the latter indicated gain in performance through increase of diversity order (2-4 dB gain). An immediate conclusion is a suggestion on adaptation of wavelength diversity when coherent receivers . The investigation also evaluated the capacity and outage of fast and slow fading channels with parameters motivated by the channel modelling work. The shaping gain was evaluated and an LDPC code design example was provided for FSO downlinks. Finally, TFP enabled a remarkable performance gain when applied to coherent detection schemes, but only marginal with direct detection. The paper concludes by pointing to the next steps that build on this investigation and the need to corroborate with measurements.**

I. Introduction

In single-mode fiber-optics transmissions, coherent optical systems, already investigated in early nineties, were lately abandoned when the advent of optical amplifiers favored the development and spreading of intensity-modulation/direct-detection (IM/DD) systems (e.g., see [1], [2] and references therein). At the beginning of this century, however, the ever increasing data rates have stimulated a renewed interest toward coherent systems since they present many advantages [3] including the possibility to adopt high-order modulations, the absence of information degrading nonlinear transformations at the receiver, the possibility to perfectly compensate for group velocity dispersion (GVD) and polarization mode dispersion (PMD) through a simple feedforward equalizer, the availability of advanced signal processing techniques (e.g., single- and multi-carrier predistortion, equalization) to compensate for the possible impairments and the possibility to adopt sophisticated state-of-the-art techniques like time-frequency packing (TFP) [4]–[8], probabilistic constellation shaping [9], [10], polarization multiplexing [3], orthogonal frequency-division multiplexing [11] among others.

The evolution experienced by fiber-optics systems and networks and the maturity of optical coherent technologies can have a significant impact also in free-space optics (FSO) technology currently based on IM/DD systems [12], [13]. The first recommended standard released by the Consultative Committee for Space Data Systems (CCSDS) optical working group (OPT), deals with the coding and synchronization layer of high photon efficiency (HPE) links such as the ones encountered in deep space missions [12]. It is based on pulse position modulation. The next step for the CCSDS OPT standardization effort is targeting the design of the coding and synchronization layer of a waveform supporting optical low Earth orbit (LEO) direct-to-Earth (DTE) links at a 1550 nm wavelength, and will rely on optical on-off keying (O3K) providing channel data rates from few Mbps up to 10 Gbps [13].

Among the several works considering IM/DD FSO, system studies for MEO and GEO with optical feeder uplinks have been conducted in [14], [15]. A detailed modelling of the optical transmitter characteristics, channel, receiver optical-electrical conversion has been considered along with an optical ground segment network dimensioning in these works. The nature of the link, technology and complexity of the payload led to the use of IM/DD for FSO. On the other hand, for the space-ground downlink from LEO, an Adaptive Optics (AO)

set-up followed by digital processing has been considered in a recent work toward coherent optical communications [16]. A perusal of the literature indicates that a key fiber optic technology that can be investigated for FSO is the coherent transmission. This is motivated by the recent work [16] and the first challenge is to consider scenarios in FSO amenable for coherent transmissions and enabling the same. Subsequently, the aim of the present activity is to investigate whether some of the more recent technologies adopted in state-of-the-art coherent fiber-optics systems could find applications in FSO systems.

II. Scenario and Channel Model

A. FSO Scenario

The study considers two scenarios

- Inter-satellite links (ISL) among the existing and emerging non-GEO constellations and the transmission in this scenario involves, ideally, a non-disruptive medium benign to achieve coherence.
- High-end links between LEO/MEO/GEO and the ground with relatively large satellite platforms [15] where the transmission is through a disruptive medium.

The FSO channel modelling is an essential step to design efficient optical communication links. Several works has attempted to describe the effect of the FSO channel on the transmitted optical beam and a summary is presented below.

B. FSO channel models

The optical power launched from the transmitter is affected by various factors before arriving at the receiver. Besides the system loss that is highly depending on the design specifications, the main effect is related to the atmosphere. In this context, the channel degradation is caused by : (1) atmosphere particles leading to loss of light energy, and (2) inhomogeneities in the temperature and the pressure of the atmosphere leading to fading. In the following, we will focus on the second effect (i.e., fading) and we will assume a clear atmosphere conditions.

1) Atmospheric turbulence: The temperature and pressure instability (mainly caused by solar heating and wind) within the earth's atmosphere produces a state of turbulence. This causes fluctuations in the index of refraction known as *scintillations* and their intensity depends on temperature, pressure, distance between the transmitter and receiver among others. The refractive index structure parameters C_n^2, quantifies the scintillation and is a function of altitude, time of day, year, and local atmospheric conditions [17]. Another important parameter is the scintillation index σ_I^2, defined as,

$$\sigma_I^2 = \frac{\mathbf{E}\{I^2\}}{\mathbf{E}\{I\}^2} - 1, \tag{1}$$

where I is the intensity of the received optical wave and $\mathbf{E}$ denotes the expected value. The intensity-fluctuation varies randomly with time. Several works have attempted to describe this stochastic processes by the definition of its statistics. Consequently, several statistical channel models have been proposed [18], but the most widely accepted models are: the lognormal distribution [19], [20], negative exponential distribution [21], [22], K distribution [23], and Gamma-Gamma distribution [19], [22]. Further, some works also model the phase variations using a Gaussian distribution [17], [24]–[26].

2) Satellite-to-ground FSO channel models: It was shown in [19] that the σ_I^2 varies with zenith angle. Weak fluctuation can be assumed only for zenith angles less than 60 deg, when ground level turbulence is of the order of $C_n^2(0) = 1.7 \times 10^{-14} m^{-2/3}$. For larger zenith angles, moderate-to-strong irradiance fluctuations need to be considered. With regards to the fade statistics, measurements of intensity scintillationsand wave-front distortions performed for laser downlinks from a LEO satellite (i.e. Japanese Optical Inter-orbit Communications Engineering Test Satellite) to the DLR Optical Ground Station has shown that the optical beam statistics depend on the elevation angle and varies from Gaussian to log-normal. Similarly, the phase statistics depend on the elevation. Finally, the channel coherence time is typically 0.1 to 10 ms [27] and is confirmed by the measurements done in [28], [29].

3) Inter-Satellite Link: With regards to the propagation channel, assuming the requirements on pointing/tracking are met and ignoring the free-space loss, the channel is seen to be flat and less complex due to vacuum as medium. Compared to fiber optics the signal will not be distorted by any non-linearity [30]. However, due to relative motion between satellites constituting the ISL, the channel is considered to be *fast-varying channel* with a non-negligible Doppler effect. In this context, a precompensation involving calculating the Doppler shift and adjusting the lasers based on satellite location, followed by the use of optical phase-locked loops (OPLL) is considered as a solution to overcome frequency mismatch and perform carrier recovery [30], [31].

4) Difference with fiber-optics: The impairments characterizing the space-based FSO scenarios are strongly different from those related to fiber-optics systems. In fact, fiber-optics systems experience nonlinear effects, due to the presence of distributed optical amplification, GVD, and PMD. If GVD and PMD are absent in FSO systems, nonlinear amplification can only occur at the transmitter. On the other hand, FSO systems involving propagation through the atmosphere, will experience turbulence which is an effect more similar to flat fading in wireless RF systems. According to [32], the atmospheric turbulence causes random fluctuations in both the amplitude and the phase of the received signal. This results in a considerable degradation of the system performance, especially in long-distance transmissions.

III. Receiver Architecture

The current generation of long-haul fiber-optics systems is based on coherent technology, that enables the adoption of high order modulations. In addition, polarization multiplexing is employed, so that two independent sequences of coded complex symbols are transmitted, after linear modulation, on two orthogonal states of polarization (SOPs).

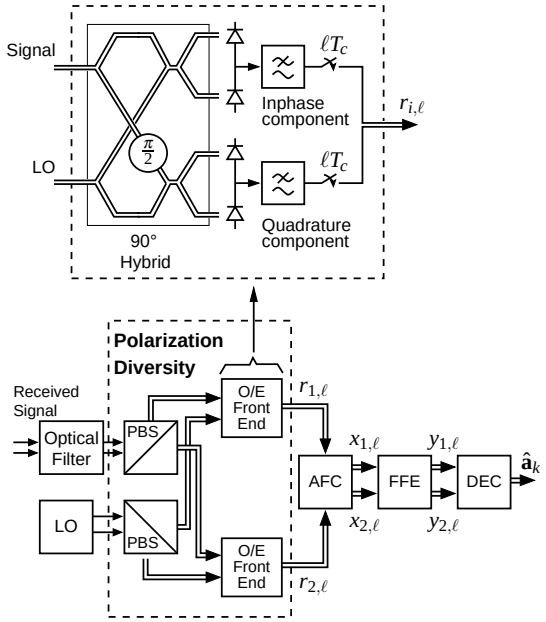

Fig. 1. Coherent receiver structure.

In a FSO transmission system, the major difference with respect to a fiber optics system is the absence of Kerr effect. This brings both favourable and limiting implications since, on one side, no nonlinear distortions such as self- or cross-phase modulation occur while, on the other hand, it is not possible to conceive nonlinear optical signal manipulations, such as, e.g., lossless polarization attraction that is based on the nonlinear Cross-Polarization Modulation [33]–[35]. We will thus assume a link without nonlinear distortions and that the transmitted signal is optically amplified before the receiver. No matter if a semiconductor optical amplifier (SOA) or an erbium doped fiber amplifier (EDFA) is used, we can assume that the dominant source of noise, besides thermal and shot noise, is the amplified spontaneous emission (ASE).

As depicted in Fig. 1, the receiver is composed of an analog part, the opto-electronic (O/E) front end, devoted to signal demodulation and conversion from the optical to the electrical domain, and a digital part devoted to electronic processing. After a preliminary optical filtering, two orthogonal SOPs are split through a polarization beam slitter (PBS). They are then separately combined with the optical field of a local oscillator laser (LO) in a 2×4 $90°$ hybrid [36] and detected with two balanced photodetectors. In this way, the two received signals, one for each SOP, are converted to the electrical domain. The received signal can be expressed as

$$\mathbf{r}(t) = [r_1(t), r_2(t)]^T = \sum_{\ell} \mathbf{H}(t - \ell T)\mathbf{a}_\ell e^{j2\pi Ft} + \mathbf{w}(t) \quad (2)$$

where $\mathbf{a}_\ell$ are the (2×1) symbols, $F \leq 1/T$ is the frequency offset between the incoming signal and the local oscillator, and $\mathbf{H}(t)$ is the 2×2 Jones matrix representing the impulse response of the linear transmission channel, that accounts for both linear distortions and a possible constant unknown phase shift due to the phase uncertainty between the transmit and receive lasers. Finally, $\mathbf{w}(t) = [w_1(t), w_2(t)]^T$ are the low-pass equivalent of the ASE noise components on the orthogonal SOPs, that can be modeled as a couple of independent complex processes, each with two-sided power spectral density (PSD) equal to N_0.

The processing that follows in the receiver is assumed to be fully digital. To this purpose, a possible way of extracting sufficient statistics from the received signal $\mathbf{r}(t)$ is by means of sampling at the Nyquist rate [37]. If η samples per symbol interval T are extracted from the signal, the sampling interval is $T_c = T/\eta$ and the number of samples depends on the bandwidth of the received useful signal and the value of F. We assume that the optical filter has no effect on the useful signal and that the electrical filters in Fig. 1 have squared amplitude response with vestigial symmetry around $\eta/2T$ [37]. This latter condition ensures that the noise samples are independent and identically distributed complex Gaussian random variables with mean zero and variance $\sigma^2 = N_0\eta/T$ [37]. The samples of $\mathbf{r}(t)$ at discrete-time instants are denoted as $\mathbf{r}_\ell = \mathbf{r}(\ell T_c) = [r_{1,\ell}, r_{2,\ell}]^T$.

The fine frequency recovery is then performed by means of an electrical AFC loop which performs closed-loop frequency estimation and compensation assuming that neither data nor clock information is available. An adaptive two-dimensional fractionally-spaced feed-forward equalizer (FFE) of sufficient length is then able to perfectly compensate for all linear impairments that are present in the channel, thus allowing a simple classical symbol-by-symbol detection. In the presence of phase noise, a more robust symbol-by-symbol detection strategy with decision-feedback can be devised instead.

IV. Time-Frequency Packing

In transmission systems the orthogonality condition sets a lower limit to time- and frequency-spacing (the Nyquist criterion), such that the achievable spectral efficiency (SE) is limited by the number of levels of the underlying modulation format. A different approach, giving up the orthogonality condition, allows to overcome the Nyquist limit and achieve a higher SE with low-order modulations [38], [39]. This time- and frequency-packing (TFP) approach is an extension of the well known faster-than-Nyquist (FTN) signaling [40]. Rather than as a specific modulation format, TFP should be regarded as a design procedure for the optimization of a class of modulation formats—namely, multicarrier linear modulations.

All the equally-spaced carriers are linearly modulated with the same modulation format and shaping pulse $p(t)$. The complex envelope of the transmitted signal is

$$\mathbf{x}(t) = \sum_{\ell=-M}^{M} \sum_{k=1}^{K} \mathbf{x}_k^{(\ell)} p(t - kT) e^{j2\pi \ell F t} \quad (3)$$

where $\mathbf{x}_k^{(\ell)}$ is the transmitted symbol (a two-component vector, one per each polarization, in coherent optical communications) on the ℓ-th carrier at time kT, T is the symbol time (or time spacing between adjacent symbols), F the frequency spacing

between adjacent carriers, and, for simplicity, a perfect time and phase synchronization among the carriers is assumed. Signal (3) is corrupted by additive white Gaussian noise (AWGN) and demodulated by a bank of matched filters and symbol-time samplers. Assuming a system with a sufficiently large number of carriers $2M+1$ to neglect border effects and denoting by $\mathbf{x} = \{\mathbf{x}_k^{(\ell)}\}$ the set of transmitted symbols and by $\mathbf{y} = \{\mathbf{y}_k^{(\ell)}\}$ the set of channel outputs, the SE of the system (bit/s/Hz) is

$$\eta = \frac{I(\mathbf{X};\mathbf{Y})}{FT} \tag{4}$$

where $I(\mathbf{X};\mathbf{Y})$ is the average mutual information rate (IR) (bit/symbol) between input and output. If we give up the orthogonality condition, we have no constraints on the choice of $p(t)$, F, and T. Thus, we can select a shaping pulse $p(t)$ and increase (4) by reducing the denominator FT below the Nyquist limit. This way, however, we also introduce intercarrier and intersymbol interference (ICI and ISI) and, therefore, reduce the IR. TFP seeks the best solution by dividing the problem in three parts: i) set the desired input constellation and detector complexity; ii) find the optimum T and F spacing which provide the maximum achievable SE (ASE) for the given input constellation and detector complexity; iii) select a proper code to approach as close as desired the achievable SE (ASE).

By exploiting the mismatch decoder principle [41] and the auxiliary channel approach [42], the achievable IR (AIR) and ASE can be efficiently evaluated through simulations, in terms of lower bounds. The maximum ASE depends on the given SNR (it increases as the SNR increases), but the optimum F and T depend only slightly on it, such that a single optimization can be adopted for a wide range of SNRs (i.e., of link distances).

The last step of the TFP method is common to almost any digital communication system and consists in finding a coding strategy, by taking into account the peculiarities related to the presence of ISI and ICI. Thus, a custom design of the code is often required.

As concerns the simulated systems, we focused on coherent detection with quadrature phase shift keying (QPSK) format, and in this case we also considered a higher-complexity MAP detector (a BCJR [43]); on the other hand, we also envisaged a simpler IM/DD system, employing a four-level pulse amplitude modulation (4PAM), but in this case only cheaper symbol-by-symbol receivers with minimum mean square error (MMSE) equalization were accounted for. Fig. 2 shows the performance in terms of ASE of the QPSK and 4PAM formats, for the number of trellis states from 1 to 256 and with roll-off equal to 0.1 in an AWGN scenario. It can be noticed that a remarkable performance increase can be obtained with coherent detection, actually amounting to almost 250% with respect to the Nyquist case.[1]

[1]Similar results can be obtained with coherent higher-level quadrature amplitude modulation (QAM), namely 16QAM, and IM/DD on-off keying (OOK).

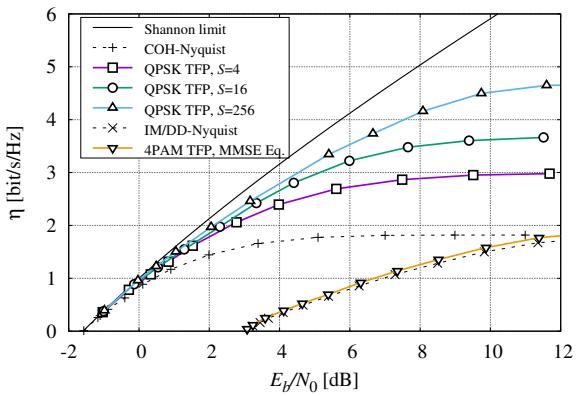

Fig. 2. ASE of coherent (COH) QPSK with different detector complexity and of 4PAM IM/DD with MMSE equalizer.

The benefits of TFP with IM/DD, on the contrary, are almost negligible. Actually, given the low complexity detector employed, only a very limited spacing optimization is possible with this format, therefore TFP for this kind of front-end can be considered not to be particularly useful.

In order to take into account the fading channel due to atmospheric turbolence, the outage capacity was considered, which depends on the selected outage probability, and on the distribution of the received power, which in turn depends on the elevation angle. Thus, in Fig. 3 we derived the SNR penalty as a function of the elevation angle, and of three different values of outage probability, when the power scintillation index is $\sigma_I^2 = 0.1$ (i.e., moderate atmospheric turbulence), for coherent and IM/DD respectively (the latter is basically twice the former). It can be noticed that for low-elevation angles the penalty is remarkable, but, however, the performance is only related to the type of receiver, be it coherent or non-coherent, and not to the particular technique/modulation employed. Ultimately, it can be said that TFP with coherent detection, and more specifically with the QPSK format, offers a favorable trade-off between flexibility and hardware complexity, given the quite simple transmitter architecture and the possibility to easily adapt system parameters to the scenario at hand, via software defined configuration of digital filtering and receiver processing complexity.

V. Capacity Analysis

To model transmission from a low earth orbit (LEO) satellite to ground, we consider the following simplified discrete-time channel model [22], [26]

$$y = \sqrt{h}x + n. \tag{5}$$

where y is the received symbol, x the transmitted symbol, h the power gain, n the additive white Gaussian noise (AWGN) noise. Let the capacity C be defined as the maximum mutual information (MI) between the channel input X and channel output Y, i.e.,

$$C = \max_{P(x)} I(X;Y) \tag{6}$$

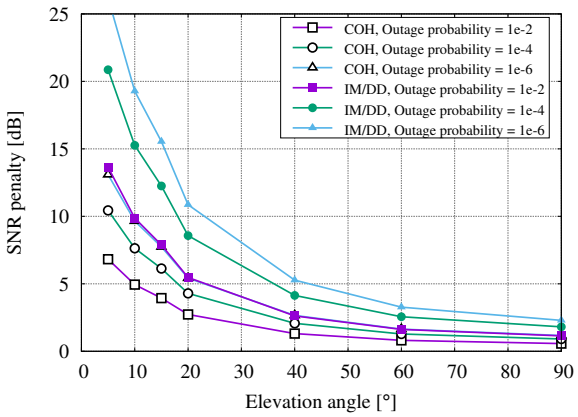

Fig. 3. Outage capacity SNR penalty for coherent (COH) and IM/DD.

For an ergodic fading channel capacity C_{ff} is

$$C_{ff} = \max_{P(x)} \int_0^\infty I\left(X;Y|H=h\right) p(h)\, \mathrm{d}h. \tag{7}$$

The MI $I\left(X;Y|H=h\right)$ in (7) corresponds to the MI of an AWGN channel with signal-to-noise ratio (SNR) $\gamma = h\frac{E_s}{N_0}$ where γ is also referred to as instantaneous SNR.

For non-ergodic channels, capacity computations turn out to be numerically cumbersome. A simplified approximation of channels with memory is the block fading channel which is a widely adapted for terrestrial wireless systems. They rely on the assumption that the channel gain is constant over one block of transmission, but independent and identically distributed (i.i.d.) over various blocks. We use the simplified block fading channel model to analyze the outage capacity of free-space optical (FSO) links. Since the channel gain, and thus the instantaneous MI are random variables (r.v.s) we define the outage probability as the probability that the transmission rate R exceeds the average instantaneous MI over L blocks, i.e.,

$$p_{\mathsf{out}}(R) = \Pr\left\{\max_{P(x)} \frac{1}{L}\sum_{\ell=1}^{L} I(X,Y,H_\ell) < R\right\} \tag{8}$$

The ϵ-outage capacity C_ϵ for the block fading channel is

$$C_\epsilon = \operatorname*{argmax}_R\, p_{\mathsf{out}}(R) < \epsilon. \tag{9}$$

In average error free communication is possible with rate

$$\bar{R}_\epsilon = (1-\epsilon)C_\epsilon. \tag{10}$$

The parameter L is called diversity order of the system.

For current FSO systems the repetition of the signal (possibly) with maximum ratio combining (MRC) at the receiver is a common strategy to increase the diversity order of the system. Capacity computations can be extended in a straight forward manner to this case. For MRC , the distribution of the channel gain is changed according to the transformation

$$H_{MRC} = \sum_{t=1}^{T} H_t \tag{11}$$

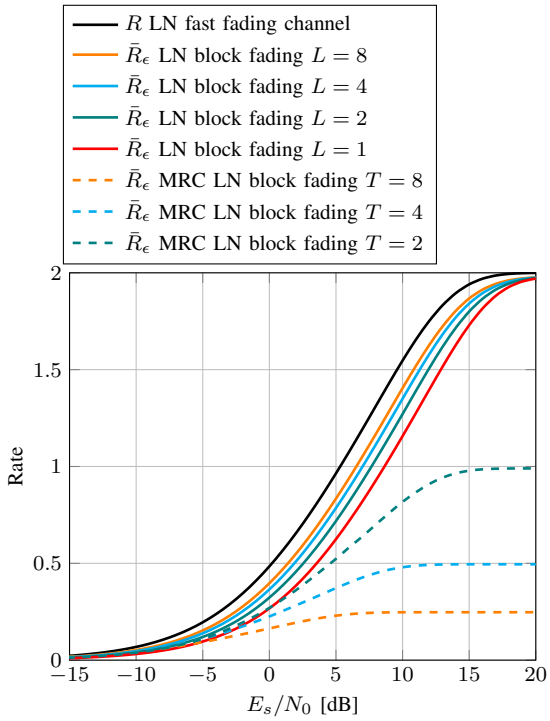

Fig. 4. Rates LN block fading channel (uniform) with repetition and MRC with $s_h^2 = 0.1$, 4-ASK, $\epsilon = 0.01$.

where T is the number of transmissions/repetitions. The r.v. H_{MRC} is used in (8) to compute an outage probability for this case out of which an ϵ-outage capacity can be derived. The overall rate becomes

$$\bar{R}_\epsilon = \frac{1}{T}(1-\epsilon)C_\epsilon. \tag{12}$$

For LEO downlinks the power gain is log-normal (LN) distributed. The LN distribution can be described by two parameters, the mean m_h and variance s_h^2 of the underlying normal distribution. For $\mathrm{E}[H] \stackrel{!}{=} 1$, $m_h = -\frac{s_h^2}{2}$ and have $s_h^2 = \ln(1+\sigma_I^2)$. [44] provides representative values of the power scintillation index σ_I^2. Figure 4 illustrates rates for $s_h^2 = 0.1$ which is typical for LEO downlinks with weak turbulence, an elevation of 10°, a wavelength of 847 nm, and an aperture size of 40 cm.

VI. Conclusions

The work studied the use of pertinent FO techniques for the FSO with an aim of enhancing the synergies between the two and leveraging on technological maturity. The work identified the key system differences between the two systems. Particularly, the FSO channel model, receiver architectures (with emphasis on coherent receiver) and diversity schemes were investigated. An immediate conclusion is a suggestion on adaptation of wavelength diversity when coherent receivers. The work also evaluated the capacity and outage of fast and slow fading channels with parameters motivated by the channel modelling work. Finally TFP enabled a remarkable

performance gain when applied to coherent detection schemes, but only marginal with direct detection.

REFERENCES

[1] T. Foggi, E. Forestieri, G. Colavolpe, and G. Prati, "Maximum likelihood sequence detection with closed-form metrics in OOK optical systems impaired by GVD e PMD," *J. Lightwave Tech.*, vol. 24, no. 8, pp. 3073–3087, Aug. 2006.

[2] G. Colavolpe, T. Foggi, E. Forestieri, and G. Prati, "Multilevel optical systems with MLSD receivers insensitive to GVD and PMD," *J. Lightwave Tech.*, vol. 26, pp. 1263–1273, May 15 2008.

[3] ——, "Robust multilevel coherent optical systems with linear processing at the receiver," *J. Lightwave Tech.*, vol. 27, no. 13, pp. 2357–2369, July 1 2009.

[4] A. Barbieri, D. Fertonani, and G. Colavolpe, "Time-frequency packing for linear modulations: spectral efficiency and practical detection schemes," *IEEE Trans. Commun.*, vol. 57, pp. 2951–2959, Oct. 2009.

[5] G. Colavolpe, T. Foggi, A. Modenini, and A. Piemontese, "Faster-than-Nyquist and beyond: how to improve spectral efficiency by accepting interference," *Opt. Express*, vol. 19, no. 27, pp. 26 600–26 609, Dec 2011. [Online]. Available: http://www.opticsexpress.org/abstract.cfm?URI=oe-19-27-26600

[6] G. Colavolpe and T. Foggi, "Time-frequency packing for high capacity coherent optical links," *IEEE Trans. Commun.*, vol. 62, pp. 2986–2995, Aug. 2014.

[7] T. Foggi, G. Colavolpe, A. Bononi, and P. Serena, "Spectral efficiency optimization in flexi-grid long-haul optical systems," *J. Lightwave Tech.*, vol. 33, no. 13, pp. 2735–2742, 2015.

[8] M. Secondini, T. Foggi, F. Fresi, G. Meloni, F. Cavaliere, G. Colavolpe, E. Forestieri, L. Potì R. Sabella, and G. Prati, "Optical time-frequency packing: principles, design, implementation, and experimental demonstration," *J. Lightwave Tech.*, vol. 33, no. 17, pp. 3558–3570, Sept. 1 2015.

[9] G. Böcherer, F. Steiner, and P. Schulte, "Bandwidth efficient and rate-matched low-density parity-check coded modulation," *IEEE Transactions on Communications*, vol. 63, no. 12, pp. 4651–4665, 2015.

[10] P. Schulte and G. Böcherer, "Constant composition distribution matching," *IEEE Transactions on Information Theory*, vol. 62, no. 1, pp. 430–434, 2016.

[11] A. Barbieri, G. Colavolpe, T. Foggi, E. Forestieri, and G. Prati, "OFDM vs. single-carrier transmission for 100 Gbps optical communication," *J. Lightwave Tech.*, vol. 28, no. 17, pp. 2537–2551, September 1 2010.

[12] CCSDS, 142.0-B-1, *Recommended standard - Optical Communications Coding Synchronization*, August 2019.

[13] CCSDS, 141.0-B-1, *Recommended standard + Pink Sheets for O3K - Optical Communications Physical Layer*, February 2020.

[14] A. Mengali, C. Kourogiorgas, N. Lyras, B. S. M. R, A. Panagopoulos, and K. Liolis, *Optical Feeder Links Study towards Future Generation MEO VHTS Systems*, 2017, p. 5411.

[15] A. Mengali, C. I. Kourogiorgas, N. K. Lyras, B. Shankar Mysore Rama Rao, F. Kayhan, A. D. Panagopoulos, T. Bäumer, and K. Liolis, "Ground-to-GEO optical feeder links for very high throughput satellite networks: Accent on diversity techniques," *International Journal of Satellite Communications and Networking*, 2020.

[16] L. Paillier, R. Le Bidan, J.-M. Conan, G. Artaud, N. Védrenne, and Y. Jaouën, "Space-ground coherent optical links: Ground receiver performance with adaptive optics and digital phase-locked loop," *Journal of Lightwave Technology*, vol. 38, no. 20, pp. 5716–5727, 2020.

[17] K. A. Winick, "Atmospheric turbulence-induced signal fades on optical heterodyne communication links," *Applied optics*, vol. 25, no. 11, pp. 1817–1825, 1986.

[18] M. A. Khalighi and M. Uysal, "Survey on free space optical communication: A communication theory perspective," *IEEE communications surveys & tutorials*, vol. 16, no. 4, pp. 2231–2258, 2014.

[19] L. C. Andrews and R. L. Phillips, "Laser beam propagation through random media." SPIE, 2005.

[20] V. I. Tatarski, *Wave propagation in a turbulent medium*. Courier Dover Publications, 2016.

[21] L. C. Andrews, R. L. Phillips, and C. Y. Hopen, *Laser beam scintillation with applications*. SPIE press, 2001, vol. 99.

[22] A. Al-Habash, L. C. Andrews, and R. L. Phillips, "Mathematical model for the irradiance probability density function of a laser beam propagating through turbulent media," *Optical engineering*, vol. 40, no. 8, pp. 1554–1562, 2001.

[23] E. Jakeman and P. Pusey, "Significance of k distributions in scattering experiments," *Physical Review Letters*, vol. 40, no. 9, p. 546, 1978.

[24] J. H. Churnside and C. M. McIntyre, "Signal current probability distribution for optical heterodyne receivers in the turbulent atmosphere. 1: Theory," *Applied optics*, vol. 17, no. 14, pp. 2141–2147, 1978.

[25] N. Perlot, "Turbulence-induced fading probability in coherent optical communication through the atmosphere," *Applied optics*, vol. 46, no. 29, pp. 7218–7226, 2007.

[26] A. Belmonte and J. M. Kahn, "Performance of synchronous optical receivers using atmospheric compensation techniques," *Optics express*, vol. 16, no. 18, pp. 14 151–14 162, 2008.

[27] V. W. Chan, "Free-space optical communications," *Journal of Lightwave technology*, vol. 24, no. 12, pp. 4750–4762, 2006.

[28] F. Moll and M. Knapel, "Free-space laser communications for satellite downlinks: Measurements of the atmospheric channel," *Proceedings of IAC2011*, 2011.

[29] D. Giggenbach, F. Moll, and N. Perlot, "Optical communication experiments at dlr," *Journal of the National Institute of Information and Communications Technology*, vol. 59, no. 1/2 March/June 2012, pp. 125–134, 2012.

[30] S. Schaefer, M. Gregory, and W. Rosenkranz, "Numerical investigation of a free-space optical coherent communication system based on optical phase-locked loop techniques for highspeed," in *Photonic Networks; 16. ITG Symposium*. VDE, 2015, pp. 1–6.

[31] T. Ando, E. Haraguchi, K. Tajima, Y. Hirano, T. Hanada, and S. Yamakawa, "Coherent homodyne receiver with a compensator of doppler shifts for inter orbit optical communication," in *Free-Space Laser Communication Technologies XXIII*, vol. 7923. International Society for Optics and Photonics, 2011, p. 79230J.

[32] M. A. Khalighi and M. Uysal, "Survey on free space optical communication: A communication theory perspective," *IEEE Communications Surveys & Tutorials*, vol. 16, no. 4, pp. 2231–2258, 2014.

[33] M. Barozzi, A. Vannucci, and D. Sperti, "Lossless polarization attraction simulation with a novel and simple counterpropagation algorithm for optical signals," *Journal of the European Optical Society - Rapid publications*, vol. 7, Oct 2012.

[34] M. Barozzi and A. Vannucci, "Performance characterization and guidelines for the design of a counter-propagating nonlinear lossless polarizer," *J. Opt. Soc. Am. B*, vol. 30, no. 12, pp. 3102–3110, Dec 2013.

[35] ——, "Dynamics of lossless polarization attraction," *Photon. Res.*, vol. 3, no. 5, pp. 229–233, Oct 2015.

[36] L. G. Kazowsky, S. Benedetto, and A. Willner, *Optical Fiber Communication Systems*. Norwood, MA: Artec House, 1996.

[37] H. Meyr, M. Oerder, and A. Polydoros, "On sampling rate, analog prefiltering, and sufficient statistics for digital receivers," *IEEE Trans. Commun.*, vol. 42, pp. 3208–3214, Dec. 1994.

[38] A. Barbieri, D. Fertonani, and G. Colavolpe, "Improving the spectral efficiency of linear modulations through time-frequency packing," in *Proc. IEEE International Symposium on Information Theory*, Toronto, Canada, Jul. 2008, pp. 2742–2746.

[39] G. Colavolpe and T. Foggi, "Next-generation long-haul optical links: higher spectral efficiency through time-frequency packing," in *Proc. IEEE Global Telecommun. Conf.*, vol. 1, Dec. 2013.

[40] J. E. Mazo, "Faster-than-Nyquist signaling," *Bell System Tech. J.*, vol. 54, pp. 1450–1462, Oct. 1975.

[41] N. Merhav, G. Kaplan, A. Lapidoth, and S. Shamai, "On information rates for mismatched decoders," *IEEE Trans. Inform. Theory*, vol. 40, no. 6, pp. 1953–1967, Nov. 1994.

[42] D. M. Arnold, H.-A. Loeliger, P. O. Vontobel, A. Kavčić, and W. Zeng, "Simulation-based computation of information rates for channels with memory," *IEEE Trans. Inform. Theory*, vol. 52, no. 8, pp. 3498–3508, Aug. 2006.

[43] L. R. Bahl, J. Cocke, F. Jelinek, and J. Raviv, "Optimal decoding of linear codes for minimizing symbol error rate," *IEEE Trans. Inform. Theory*, vol. 20, pp. 284–287, Mar. 1974.

[44] M. Brechtelsbauer, D. Giggenbach, J. Horwath, M. Knapek, N. Perlot, K. Arai, T. Jono, Y. Koyama, N. Kura, and K. Ohinata, "Report on dlr-jaxa joint experiment: The kirari optical downlink to oberpfaffenhofen (kiodo)," Japan Aerospace Exploration Agency (JAXA), Tech. Rep., 2007.